The more shearing, the thicker shear band and heat-affected zone in bulk metallic glass

H. Guo and J. Wen
Shenyang National Laboratory for Materials Science, Institute of Metal Research, Chinese Academy of Sciences, Shenyang 110016, China

N.M. Xiao
Department for Special Environment Materials, Institute of Metal Research, Chinese Academy of Sciences, Shenyang 110016, China

Z.F. Zhang and M.L. Sui[a)]
Shenyang National Laboratory for Materials Science, Institute of Metal Research, Chinese Academy of Sciences, Shenyang 110016, China

(Received 17 January 2008; accepted 18 April 2008)

In a compression test for a Zr-based bulk metallic glass, a dominant shear band was preserved before fracture by a cylindrical stopper. A heat-affected zone (HAZ) ~10 μm thick together with shear band was discovered in the center of the deformed sample by preferential ion milling. By using a low aspect ratio sample for compression, diverse micron-scaled HAZs among multiple shear bands were also revealed. Based on above experimental results and the isothermal source model, it was found that the thickness of shear band and its HAZ increased continuously with the progression of shear deformation.

I. INTRODUCTION

Without slip system and dislocation-free structure in metallic glasses, shear bands often become the important plastic deformation mechanism at room temperature in bulk metallic glasses (BMGs).[1–8] The formation of free volume[3] and/or local heating[4] can cause a decrease in viscosity, leading to low plasticity and abrupt failure by shearing off along the dominant shear band. Recently, large compressive plasticity was achieved in more and more fully amorphous alloys, coming from the alloys themselves[5,6] or the external confinement condition.[7,8] In these cases, multiple shear bands are activated and the rapid propagation of shear bands is confined. These create new chances to further understand some primary properties of shear bands, including dimensions, heat release, structural change, and so on.

It is acknowledged that shear band thickness is on the order of 10 nm according to observations[9,10] and modeling.[11,12] However, the shear bands investigated in either bending[9] or in situ tension[10] experiments were created in the amorphous foils with nanometer-scaled offsets, which reflect the initial shear deformation process. Although the well-developed shear bands could be seen on surface for BMGs under loading, the offsets make it impossible to measure the thickness of shear bands exactly. So, it is still a question what is the true dimension for the well-developed shear bands in the interior of bulk samples (at least after wiping off the offset on the surface).

The local heating accompanied with the severe plastic deformation within shear bands has been observed frequently.[13–16] A large amount of heat generated will necessarily transfer from the shear band into the surrounding matrix, forming a heat-affected zone (HAZ). As important boundary conditions, the dimension and temperature of HAZ could be used to estimate the temperature rise of shear band. Using infrared imaging, Yang et al.[15] estimated a temperature rise of 333 K within the shear band by capturing a 6 μm wide HAZ with temperature rise of 0.4 K on the surface. Lewandowski and Greer[16] found the 200 to 1000 nm scaled HAZ from the local melting of the fusible-coating at 505 K, which indicated a 3400 to 8600 K temperature rise of shear band based on adiabatic model. All these results suggested that the precise magnitude of the temperature rise remained a controversial issue, strongly depending on the accurate measurement of shear band and HAZ.

As described in this article, we designed two kinds of compression experiments for the BMGs to observe the dominant shear band in the center and the multiple shear bands developed in varying degree after swiping off the offsets. Based on the analytical solution of the

[a)]Address all correspondence to this author.
email: mlsui@imr.ac.cn
DOI: 10.1557/JMR.2008.0258

one-dimensional heat conduction equation, the temperature rise during the shearing process of a Zr-based BMG was estimated.

II. EXPERIMENTAL

Amorphous alloy $Zr_{52.5}Cu_{17.9}Al_{10}Ni_{14.6}Ti_5$ was prepared by the copper mold casting method in rod and box shape, respectively. The rod sample was 3 mm in diameter with length of 50 mm. The box-shaped amorphous sample with dimensions of about 1.5 mm (height) × 3.9 (length) mm × 2.7 mm (width) was prepared for the uniaxial compressive test. The compressive strain rate is 10^{-4} s^{-1} with MTS 810 testing machine (MTS Systems Co., Eden Prairie, MN) at room temperature. The deformed samples were investigated with FEI Quanta 600 scanning electron microscope (SEM; FEI Co., Eindhoven, The Netherlands) and FEI Tecnai F30 transmission electron microscope (TEM) with point-to-point resolution of 2.0 Å, operating at 300 kV (FEI Co., Eindhoven, The Netherlands).

III. RESULTS AND DISCUSSION

The rod with 3 mm in diameter was cut into 6 mm in length for compression. Figure 1(a) shows the stress–strain curve under compressive loading, and the fracture stress reaches about 1.8 GPa with compressive plasticity below 1%. For investigating the dominant shear band, we tried to stop the localized shear before final fracture by putting a cylindrical stopper around the specimen as illustrated in Fig. 1(b). Due to the constraint of the outer cylinder, catastrophic propagation of the initiated major crack was successfully avoided. The unfractured sample with a dominant shear band was achieved, as shown in Fig. 1(c).

To check whether the compressed sample lost connection or not, it was sectioned and polished longitudinally across the shear plane. The SEM image of the cross section in Fig. 2(a) clearly shows that cracks initiated from outer surface and did not run throughout the whole sample. The bonding region between cracks seems no different compared with the matrix, although severe shearing obviously occurred there. Figure 2(b) shows a micrograph of cross-sectional specimen for TEM after grinding and dimpling but before ion milling, in which the bright loop was a copper ring. No further propagation of cracks, as shown in enlarged Fig. 2(c), suggested that the dimpling process (to shorten the ion-milling time) did not affect the sample except for some scratches on the surface. After low-voltage ion milling, the specimen penetrated at four stripe-shaped regions, marked by I to IV in Fig. 2(d). Holes I and II located at the bonding region between the cracks and shaped on the path of the cracks. The TEM bright-field image in Fig. 2(e), taken by Tecnai F30 TEM with a high tension of 300 kV, shows there is an obvious ~10 μm wide bright band locating between the cracks, which could not be observed in Fig. 2(a) by SEM. In the TEM bright-field image, the brighter intensity means that the bright band is thinner than the area elsewhere, which reflects preferential ion milling. This provides the evidence of structural changes during the shear process, just like preferential etching[17] and deformation[18] at pre-existing shear bands. Mondal et al.[19] also reported that the shear bands between cracks were visible by SEM after chemical etching.

To investigate the shear bands with different developing degrees, we achieved compressed samples with low aspect ratio. The SEM image in Fig. 3(a) shows lots of shear bands on the surface of the deformed box-shaped sample. After wiping off the offsets on the surface and twin jetting polishing, the SEM images in Fig. 3(b)

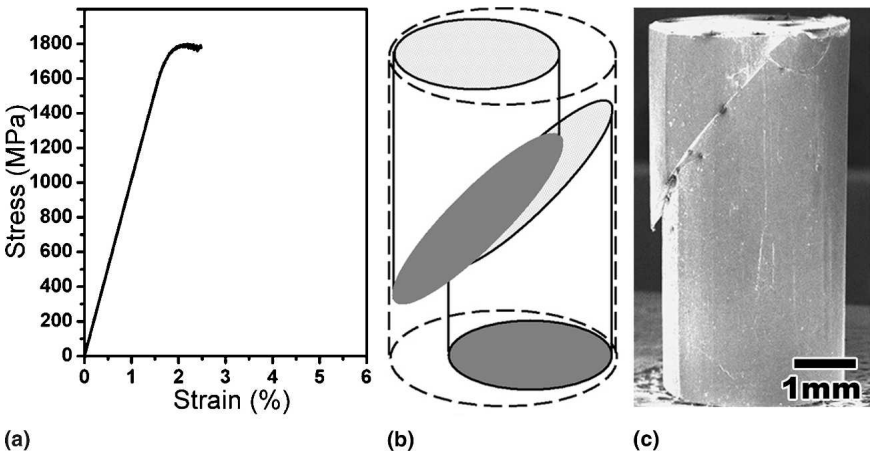

FIG. 1. (a) The stress–strain curve under compressive loading at a strain rate of 10^{-4} s^{-1}. (b) Schematic illustration of the deformed sample and the cylindrical stopper (dashed line) with 3.3 mm in diameter. (c) SEM image of the unfractured sample.

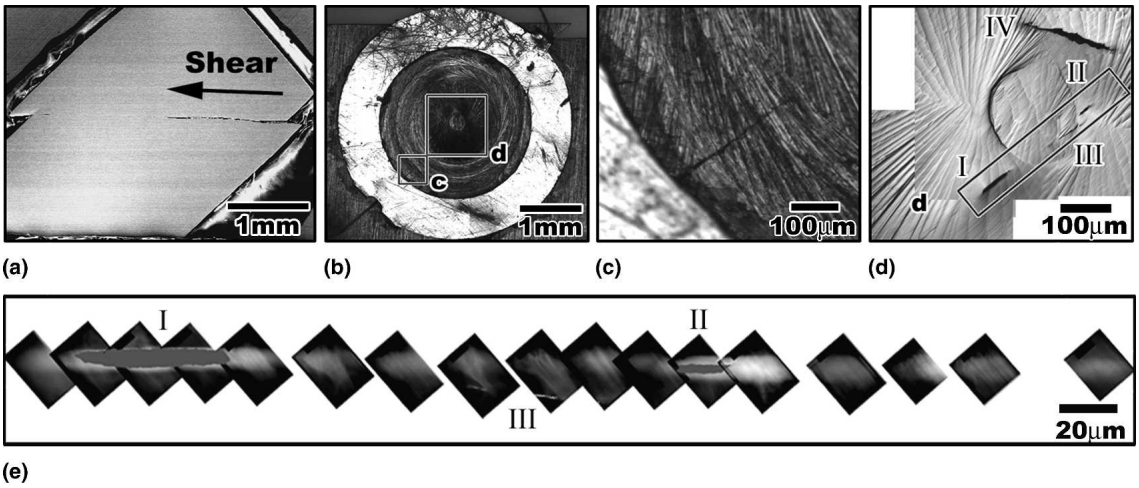

FIG. 2. (a) SEM image of the polished cross section of the compressed sample. (b) SEM micrograph of the cross-sectional specimen for TEM before ion milling. (c) The enlargement of square c in (b). (d) Corresponding to the square marked d in (b), four stripe-shaped holes penetrated after low-voltage ion milling. (e) Bright field TEM image showing a 10 μm wide bright band.

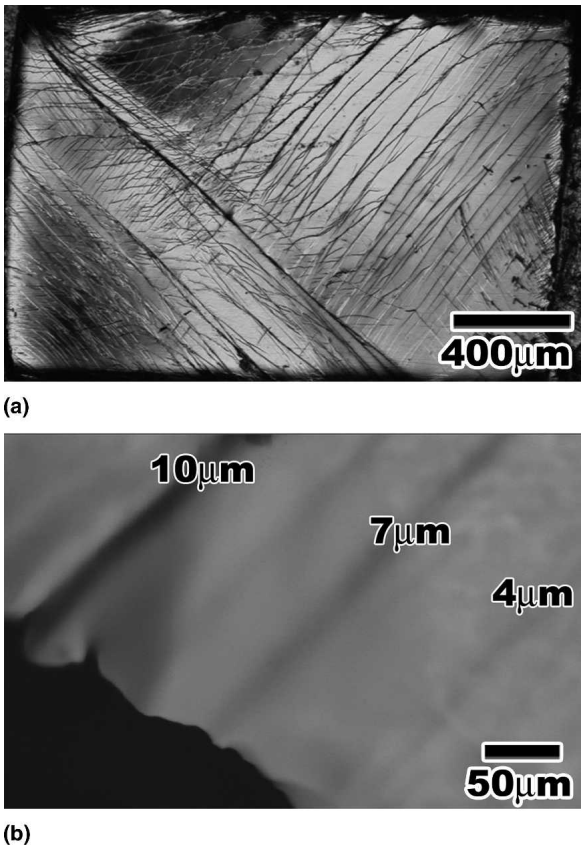

FIG. 3. (a) Multiple shear bands developed in varying degree on the surface. (b) Micron-scaled shear bands together with their HAZs after wiping off the offsets by twin jetting polishing.

clearly show a series of preferentially etched bands presenting different thickness, ranged from 4 to 10 μm. Taking the bands to intersect the surface at a shear angle of about 45°, the true thickness of bands should be 2.8 to 7.1 μm, respectively. The SEM observations on preferentially etched bands are consistent with the above TEM results.

High-resolution TEM (HRTEM) images and the corresponding diffraction patterns of matrix and preferentially ion-milled bright band were taken to inspect the structure change in bright band, as shown in Figs. 4(a) and 4(b), respectively. No difference between the HRTEM images of the matrix and the bright band can be recognized. Also, no crystallization by heat or deformation could be found in the bright band, which indicates that the ultimate elevated temperature during shear deformation should not be too much beyond the crystallization temperature (T_x) after taking the dynamic effect into consideration. Nanometer-scale defects in BMGs could be discerned using a quantitative HRTEM technique (i.e., processing HRTEM image by suitable Fourier filtering and setting image threshold).[20] However, there is no obvious difference in the nanovoid distribution between the matrix and the bright band by processing the HRTEM images (the figures are not shown here), which might be related to the shear deformation under a compression stress.[21] To investigate the structure change, fluctuation electron microscopy (FEM),[22] a recently developed electron-microscopy technique, was carried out. FEM is capable of revealing the presence of structural order on 1 to 2 nm length scale (i.e., medium-range order) in amorphous materials, for which the details of the structure are not accessible using HRTEM. It has successfully been used to characterize amorphous semiconductors[22] and BMG.[23] As shown in Fig. 4(c), FEM measurements show that the matrix had a much more pronounced peak in the variance compared with the presence of the bright band, which means that the matrix has a higher medium range order. As mentioned previously, structures of the metallic glasses can be changed by strain and heat effect during shear deformation.

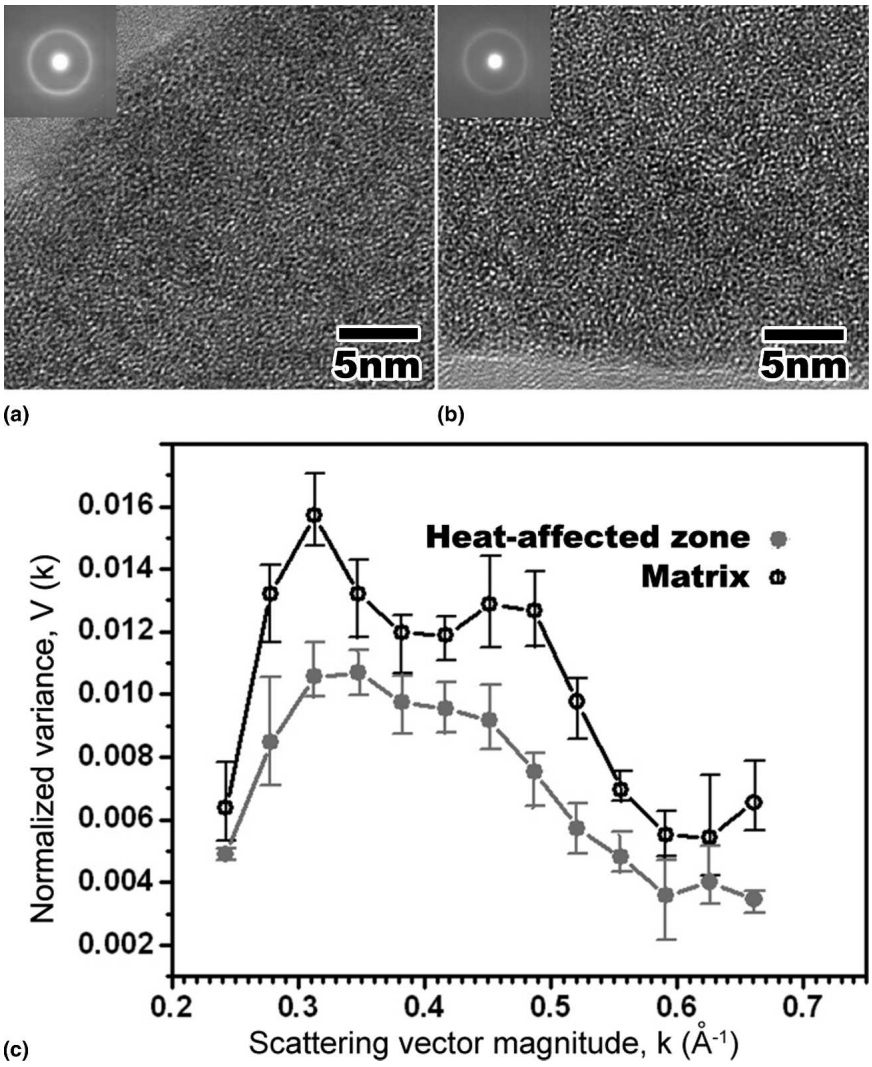

FIG. 4. HRTEM images and the electron diffraction pattern insets for (a) matrix and (b) bright band. (c) FEM result showing the structural change by $V(k)$ curves.

Considering that the 10 nm thickness of the initial shear band was far smaller than the 10 μm width of the bright band observed in the present study, the slight structure change in the bright band might be mainly affected by heat release. So, the bright band can be considered as a HAZ. For the relaxed sample (annealed at T_g), the FEM results present a similar depressed peak in variance (which was not shown here) compared with the original one, just like that for the HAZ.

The heat release from the shear bands has been discussed intensively. As noted earlier,[24] the shear band evolution was an adiabatic process, which means that all the dissipated heat in HAZ was initially confined inside the 10 nm thick shear band. Therefore, shear band could be treated as planar sources of heat, and temperature rise (ΔT_h) and thickness of the heated region have the inverse proportion.[13–16] Considering that HAZ is 1000 times wider than initial shear band in this case, the temperature rise inside the shear band will be as high as 10,000 K even taking ΔT_h as low as 10 K. Obviously, the adiabatic assumption is not reasonable, and heat conduction must take place during shear band propagation. In fact, some literature[12,15,16,24] has argued that the shear band operation could not be fully adiabatic. We supposed that at the propagation stage, shear band should be considered as an isothermal source, which remains at a certain high temperature and releases heat. A precise calculation can also be performed by solving the one-dimensional heat conduction equation:

$$\rho C_p \frac{dT}{dt} = k \frac{\partial^2 T}{\partial x^2} \quad , \tag{1}$$

where $k = 20$ W/m·K is thermal conductivity,[24] $\rho = 6.81$ g/cm^3 is the density,[12] and $C_p = 0.33$ J/g·K is the

heat capacity[25] for the current Zr-based BMG. The analytical solution of Eq. (1) is an error function and can be expressed as,

$$T(x,t) = T_s - (T_s - T_0)\mathrm{erf}\left(\frac{x}{\sqrt{4kt/\rho C_p}}\right) \quad , \qquad (2)$$

where T_s is the isothermal source temperature and T_0 is original (room) temperature. From Fig. 2(a), the offset of shear band is about 300 μm, and the whole shear time should be around 300 ns, given the velocity of shearing about 1000 m/s.[24] According to Eq. (2), given the isothermal source temperature as 1072 K (T_m),[25] the zone with the temperature rise over 100 K could reach about 3.4 μm in each side of the shear band. Also, the zones were about 2.5 and 2.7 μm wide if the temperature of heat source was taken as 675 K (T_g) and 727 K (T_x), respectively. Considering that the region with the temperature rise over 100 K would keep on broadening for a while after shearing (300 ns), it is approximately consistent with the current observation of TEM. It demonstrates that the isothermal source is more reasonable compared with fully adiabatic heating during shearing.

It should be noted that the ultimate temperature of the HAZ located in the vicinity of the initial shear band could become close to the source temperature inside the initial shear band due to the heat conduction. Considering that no boundary between the shear band and the HAZ could be identified by TEM and the stress state is similar for the shear band and the neighboring region at high temperature, the neighboring HAZ may be involved in shearing together with the initial shear band. Given the temperature of shear band could reach T_m and the region at 90% heat source temperature took part in shearing, shear band broadened with shear progression, from about 230 nm for 100 ns to 400 nm for 300 ns in each side based on Eq. (2), whereas the initial shear band was only 10 nm thick. Therefore, it is reasonable to presume that the thickness of shear band increased continuously during the shear process based on isothermal source.

At the nucleation stage of shear band, temperature rise should be adiabatic because heat completely comes from the elastic energy releasing. Temperature rise only occurs in the shearing part and the heating rate is very high. At this stage, the heat effect was limited, due to the isoconfigurational behavior. Isoconfigurational heating (at a high heating rate) could not induce the dramatic viscosity decreasing as expected in equilibrium.[26] While after forming the initial 10 nm thick shear band,[9–12] heat releasing from it made the regions in the vicinity of the initial shear band achieve a relatively high temperature. When the local temperature rose beyond some critical value, the viscosity of the metallic glass noticeably decreased and the local matrix softened to be ready for shearing. Then the shear band had no reason to refuse the neighboring atoms to join in, which reflects that the shear band continuously broadened during the shearing process. We presumed that temperature of the shear band might stay at some high value rather than keep on going up, because the less heat input from the shearing at high temperature may compensate for the heat conduction to matrix. Then, the shear band (including the initial part and the joined part) would keep on broadening at a certain high temperature by involving more of the neighboring matrix. That is, the more shearing, the thicker the shear band and its HAZ are.

IV. CONCLUSIONS

The presence of the micron-scaled HAZ around shear bands in BMGs was confirmed by TEM and SEM due to the preferential ion milling and etching. It proved that lots of heat was released in BMG alloys during the uniaxial compressive deformation. Based on an analytical solution of the one-dimensional heat conduction equation, the isothermal source is more reasonable compared with fully adiabatic heating during the shearing process. Also, the shear band and its HAZ broadened gradually as shear propagating.

ACKNOWLEDGMENTS

This work was financially supported by the National Natural Science Foundation of China (NSFC) under Grant No. 50671104 and 50625103, and the "Hundred of Talents Project" by the Chinese Academy of Sciences. Prof. M.L. Sui would like to thank Prof. E. Ma for the stimulating discussion.

REFERENCES

1. C.A. Schuh, T.C. Hufnagel, and U. Ramamurty: Mechanical behavior of amorphous alloys. *Acta Mater.* **55,** 4067 (2007).
2. A.L. Greer: Metallic glasses. *Science* **267,** 1947 (1995).
3. F. Spaepen: A microscopic mechanism for steady state inhomogeneous flow in metallic glasses. *Acta Metall.* **25,** 407 (1977).
4. H.J. Leamy, H.S. Chen, and T.T. Wang: Plastic flow and fracture of metallic glass. *Metall. Trans.* **3,** 699 (1972).
5. Y.H. Liu, G. Wang, R.J. Wang, D.Q. Zhao, M.X. Pan, and W.H. Wang: Super plastic bulk metallic glasses at room temperature. *Science* **315,** 1385 (2007).
6. Y. Zhang, W.H. Wang, and A.L. Greer: Making metallic glasses plastic by control of residual stress. *Nat. Mater.* **5,** 857 (2006).
7. Z.F. Zhang, H. Zhang, X.F. Pan, J. Das, and J. Eckert: Effect of aspect ratio on the compressive deformation and fracture behaviour of Zr-based bulk metallic glass. *Philos. Mag. Lett.* **85,** 513 (2005).
8. H. Bei, S. Xie, and E.P. George: Softening caused by profuse shear banding in a bulk metallic glass. *Phys. Rev. Lett.* **96,** 105503 (2006).
9. P.E. Donovan and W.M. Stobbs: The structure of shear bands in metallic glasses. *Acta Metall.* **29,** 1419 (1981).
10. E. Pekarskaya, C.P. Kim, and W.L. Johnson: In situ transmission

electron microscopy studies of shear bands in a bulk metallic glass based composite. *J. Mater. Res.* **16,** 2513 (2001).
11. N.P. Bailey, J. Schiøtz, and K.W. Jacobsen: Atomistic simulation study of the shear-band deformation mechanism in Mg-Cu metallic glasses. *Phys. Rev. B* **73,** 064108 (2006).
12. Y. Zhang and A.L. Greer: Thickness of shear bands in metallic glasses. *Appl. Phys. Lett.* **89,** 071907 (2006).
13. C.T. Liu, L. Heatherly, D.S. Easton, C.A. Carmichael, J.H. Schneibel, C.H. Chen, J.L. Wright, M.H. Yoo, J.A. Horton, and A. Inoue: Test environments and mechanical properties of Zr-base bulk amorphous alloys. *Metall. Mater. Trans. A* **29,** 1811 (1998).
14. W.J. Wright, R.B. Schwarz, and W.D. Nix: Localized heating during serrated plastic flow in bulk metallic glasses. *Mater. Sci. Eng., A* **319–321,** 229 (2001).
15. B. Yang, C.T. Liu, T.G. Neih, M.L. Morrison, P.K. Liaw, and R.A. Buchanan: Localized heating and fracture criterion for bulk metallic glasses. *J. Mater. Res.* **21,** 915 (2006).
16. J.J. Lewandowski and A.L. Greer: Temperature rise at shear bands in metallic glasses. *Nat. Mater.* **5,** 15 (2006).
17. C.A. Pampillo: Localized shear deformation in a glassy metal. *Scr. Metall.* **6,** 915 (1972).
18. K.D. Krishnanand and R.W. Cahn: Recovery from plastic deformation in a Ni/Nb alloy glass. *Scr. Metall.* **9,** 1259 (1975).
19. K. Mondal, G. Kumar, T. Ohkubo, K. Oishi, T. Mukai, and K. Hono: Large apparent compressive strain of metallic glasses. *Philos. Mag. Lett.* **87,** 625 (2007).
20. J. Li, Z.L. Wang, and T.C. Hufnagel: Characterization of nanometer-scale defects in metallic glasses by quantitative high-resolution transmission electron microscopy. *Phys. Rev. B* **65,** 144201 (2002).
21. W.H. Jiang and M. Atzmon: The effect of compression and tension on shear-band structure and nanocrystallization in amorphous $Al_{90}Fe_5Gd_5$: A high-resolution transmission-electron-microscopy study. *Acta Mater.* **51,** 4095 (2003).
22. M.M.J. Treacy, J.M. Gibson, and P.J. Keblinski: Paracrystallites observed in evaporated amorphous tetrahedral semiconductors. *J. Non-Cryst. Solids* **231,** 99 (1998).
23. J. Li, X. Gu, and T.C. Hufnagel: Using fluctuation microscopy to characterize structural order in metallic glasses. *Microsc. Microanal.* **9,** 509 (2003).
24. T.C. Hufnagel, T. Jiao, Y. Li, L-Q. Xing, and K.T. Ramesh: Deformation and failure of $Zr_{57}Ti_5Cu_{20}Ni_8Al_{10}$ bulk metallic glass under quasi-static and dynamic compression. *J. Mater. Res.* **17,** 1441 (2002).
25. S.C. Glade, R. Bush, D.S. Lee, W.L. Johnson, R.K. Wunderlich, and H.J. Fecht: Thermodynamics of $Cu_{47}Ti_{34}Zr_{11}Ni_8$, $Zr_{52.5}Cu_{17.9}Ni_{14.6}Al_{10}Ti_5$ and $Zr_{57}Cu_{15.4}Ni_{12.6}Al_{10}Nb_5$ bulk metallic glass forming alloys. *J. Appl. Phys.* **87,** 7242 (2000).
26. H.S. Chen and M. Goldstein: Anomalous viscoelastic behavior of metallic glasses of Pd–Si-based alloys. *J. Appl. Phys.* **43,** 1642 (1972).